Abdominal Imaging

Published online: 11 March 2014

Abdom Imaging (2014) 39:797–801
DOI: 10.1007/s00261-014-0112-2

MR imaging findings of uterine pyomyoma: radiologic–pathologic correlation

Hiromi Ono,[1] Masayuki Kanematsu,[1,2] Hiroki Kato,[1] Hiroshi Toyoki,[3] Yoh Hayasaki,[3] Tatsuro Furui,[3] Ken-ichirou Morishige,[3] Yuichiro Hatano[4]

[1]Department of Radiology, Gifu University School of Medicine, 1-1 Yanagido, Gifu 501-1194, Japan
[2]High-level Imaging Diagnosis Center, Gifu University Hospital, 1-1 Yanagido, Gifu 501-1194, Japan
[3]Department of Obstetrics and Gynecology, Gifu University School of Medicine, Gifu, Japan
[4]Department of Pathology, Gifu University School of Medicine, Gifu, Japan

Abstract

A 69-year-old postmenopausal female with a spontaneously occurring uterine pyomyoma was described with emphasis on the MR imaging findings. On unenhanced T1- and T2-weighted MR images, a huge mottled mass suspected to contain blood products, necrotic tissue, or purulent or viscous fluid was demonstrated within anterior myometrial wall of uterine body. The mass was surrounded by a peripheral rim that was hyperintense on T1-weighted images and hypointense on T2-weighted images. On gadolinium-enhanced MR images, most of the mass was unenhanced, but the peripheral rim was equally enhanced with the surrounding myometrium. Pathological examination revealed an intramural uterine pyomyoma surrounded by fibrous capsules with abundant lymphocytes and neutrophils. Our findings indicate that pyomyoma should be considered when MR images demonstrate a myometrial cystic lesion accompanied by a peripheral rim.

Key words: Pyomyoma—Suppurative leiomyoma—Uterus—MRI

Pyomyoma is clinically defined as a leiomyoma with suppurative inflammation, characterized by the production of pus or a purulent exudate that contains neutrophils and necrotic cells [1]. Most cases occur during pregnancy or after menopause, and pyomyomas that develop in postmenopausal females are presumably caused by ischemia due to hypertension, diabetes, or atherosclerosis [2]. Pyomyoma is often caused by an ascending infection from the lower genital tract and is also a rare complication of uterine artery embolization [3]. Delayed diagnosis may result in serious complications, whereas adequate surgery and broad-spectrum antibiotics may decrease serious morbidity [4]. However, these conditions may be difficult to diagnose, particularly in those with a nonspecific clinical presentation and no history of leiomyoma. Although several previous case reports have demonstrated radiographic images [1, 2, 4–7], our literature search did not reveal any report that described the detailed MR imaging findings associated with this disease. Therefore, here we describe MR imaging findings along with pathological findings of a case of pyomyoma.

Case report

A 69-year-old G3P2 postmenopausal female was presented with a 6-month history of general fatigue and pelvic discomfort. She had a 10-year history of type 2 diabetes mellitus. Laboratory examination data were notable for white blood cell counts of 10,710/μL, and C-reactive protein levels of 2.71 mg/dL. Physical examination revealed no significant findings, and her body temperature was normal.

Subsequent ultrasound (US) examinations revealed a large uterine mass with heterogeneous echogenicity. Pelvic unenhanced CT images revealed an enlarged uterus and a hypodense mass with irregular margins (Fig. 1a). The intratumoral gas was not demonstrated both on US and CT images. Moreover, sagittal T2-weighted images demonstrated a huge mottled mass with irregular margins and heterogeneously intense hyperintensity accompanied by a peripheral hypointense rim (Fig. 1b). Furthermore, sagittal T1-weighted images revealed mottled hyperintensity in the central area, suggesting the presence of blood products, necrotic tissue, or

Correspondence to: Hiromi Ono; *email:* hiromi11_br@yahoo.co.jp

purulent or viscous fluid, and the peripheral rim was clearly shown as hyperintense (Fig. 1c). Because the mass posteriorly displaced the normal endometrium on transverse images, the mass was located within anterior myometrial wall of uterine body. On sagittal gadolinium-enhanced non fat-suppressed T1-weighted images, the central area was not enhanced, but the peripheral rim seemed to be equally enhanced with the surrounding myometrium (Fig. 1d). Although preoperative radiological diagnoses included leiomyoma with red degeneration, we negative consideration to red degeneration due to lack of acute abdomen, pregnancy, and history of oral contraceptive use. Other preoperative radiological diagnoses included leiomyoma or leiomyosarcoma with cystic, myxoid, hemorrhagic, or suppurative changes.

Total hysterectomy was performed, and the excised specimen revealed a large myometrial mass containing a malodorous purulent fluid. On examination of the gross specimen, a malignant tumor was immediately suspected because of the necrotic features of the mass (Fig. 1e). Although no malignancy was revealed by the hematoxylin and eosin stain, the following was confirmed: abscess formation accompanied by an inflammatory cell infiltration including abundant histiocytes and neutrophils in the central necrotic area and surrounding fibrous capsules with abundant lymphocytes and neutrophils (Fig. 1f). The Elastic-van Gieson stain demonstrated fibrous capsules, including collagen fibers, which were stained red, whereas the normal myometrium, including smooth muscles, was stained yellow (Fig. 1g). Because a small amount of spindle cell components, which were suggestive of leiomyoma, was identified at the periphery of the mass, the final pathological diagnosis was pyomyoma. A culture of the pus revealed Pasteurella multocida.

Fig. 1. A 69-year-old-female with a pyomyoma. **A** Axial unenhanced CT image shows an enlarged uterus (*arrow*) and a hypodense mass with irregular margins (*curved arrow*). **B** Sagittal T2-weighted image shows a huge mottled mass with irregular margins and heterogeneously intense hyperintensity accompanied by a peripheral hypointense rim (*arrow*). **C** Sagittal T1-weighted image shows mottled hyperintensity in the central area, suggesting the presence of blood products, necrotic tissue, or purulent or viscous fluid. The peripheral rim is shown as clearly hyperintense. **D** Sagittal gadolinium-enhanced non fat-suppressed T1-weighted image shows a large unenhanced area and the peripheral rim of the lesion enhancing equally with the surrounding myometrium. **E** Gross specimen shows predominantly purulent material of the mass. **F** Hematoxylin and eosin stain show abscess formation (*asterisk*) accompanied by inflammatory cell infiltration including abundant histiocytes and neutrophils in the central necrotic area and fibrous capsules (*arrow*) with abundant lymphocytes and neutrophils between abscess cavity (*asterisk*) and surrounding myometrium (*star*). **G** Elastica-van Gieson stain shows fibrous capsules, including collagen fibers, which were stained *red* (*arrow*), whereas normal myometrium, including smooth muscles, was stained *yellow* (*star*). Abscess cavity (*asterisk*) is not stained.

Discussion

Uterine leiomyomas are the most common uterine neoplasms and involve smooth muscles with varying amounts of fibrous connective tissue. As leiomyomas enlarge, they may outgrow their blood supply, leading to various types of degeneration such as hyaline, myxoid, cystic, and red degeneration. On T2-weighted images, non-degenerative leiomyomas appear as well-circumscribed masses with decreased signal intensities, but degenerative leiomyomas present variable appearances [8]. In addition, hemorrhage, necrosis, and calcification may be observed [8].

In most previous reports, sonographic findings of pyomyoma were described as enlarging or heterogeneous pelvic masses with solid and cystic components. Moreover, increased echogenicity within the fluid was reported [9]. Central echogenic foci, accompanied by reverberation artifacts within the pyomyoma, were suggestive of gas-producing organisms; these were not observed with nonsuppurative diseases [5]. A further benefit of sonography is guided aspiration, which may confirm the diagnosis. Previous reports described that CT findings of pyomyoma included large unilocular or multilocular masses, and the presence of gas in a uterine leiomyoma is highly suggestive of pyomyoma [5]. Although frequency of gas formation in pyomyoma has not been determined, our literature search found only three cases of pyomyoma with intratumoral gas formation on CT images [2, 5, 7]. Moreover, characteristic CT findings of ruptured pyomyoma included gas and debris in the leiomyoma, discontinuity of leiomyoma wall, and free intraperitoneal gas and fluid [2].

On MR examination, the cystic component of pyomyoma appeared as hypointense to isointense on T1-weighted images and hypointense to hyperintense on T2-weighted images [1, 6]. These were nonspecific imaging features that were indistinguishable from those of degenerative leiomyoma or several histological types of uterine sarcoma. However, because MR imaging provides excellent soft-tissue contrast that is considerably superior to that of CT, fibrous capsules of pyomyoma may well be observed on MR images. In a previous case report of pyomyoma, MR imaging revealed a peripheral rim that appeared as hyperintense on T1-weighted images and hypointense on T2-weighted images, although a radiologic–pathologic correlation was not evaluated [1].

Because fibrous capsules of brain abscesses also appear as hyperintense on T1-weighted images and hypointense on T2-weighted images, imaging findings of pyomyoma are similar to those of cerebral abscesses. In our case, although fibrous capsules of pyomyoma were demonstrated, neither acute nor chronic hemorrhage was

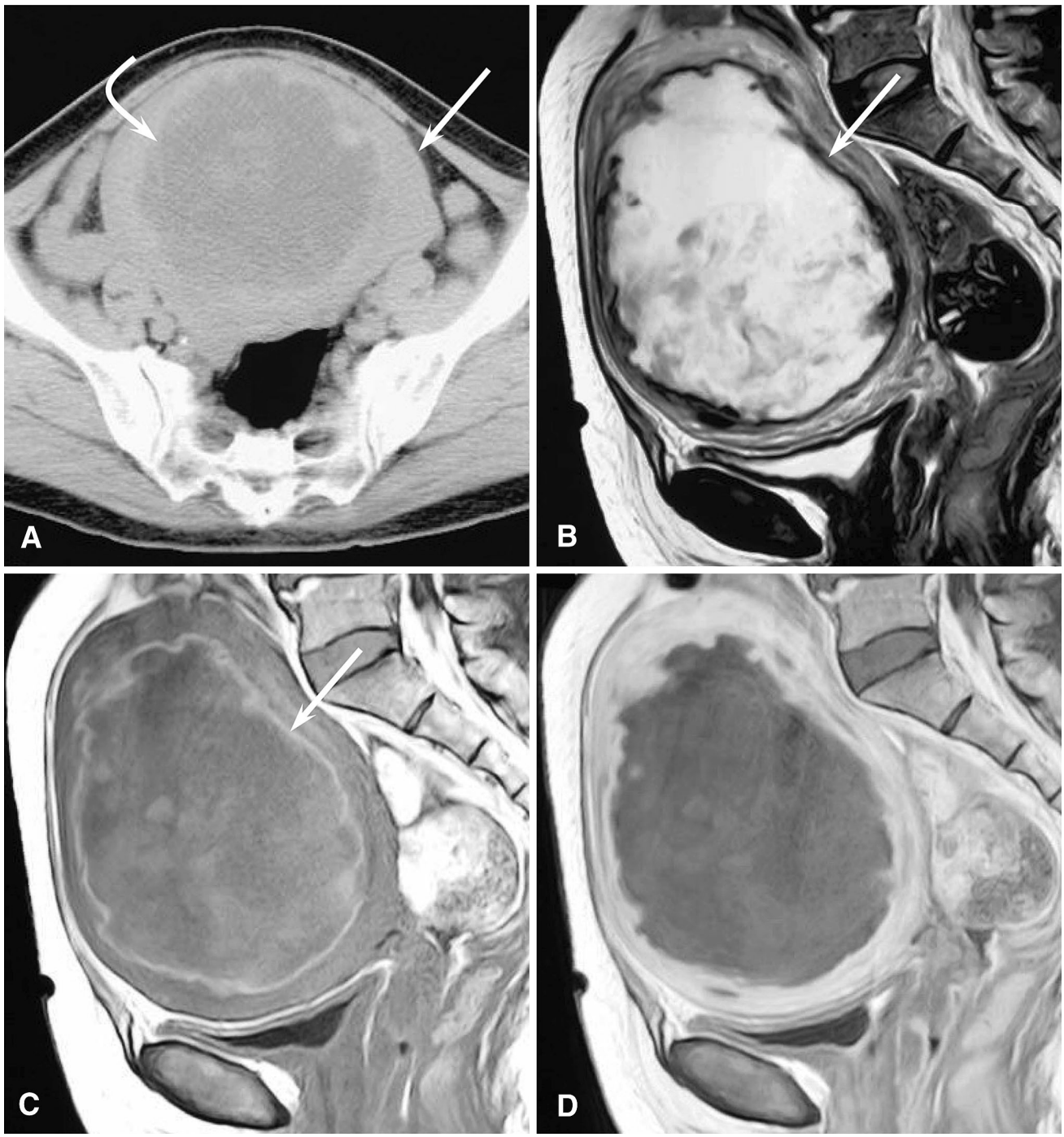

identified on pathological examination. In a previous report, unique signal intensity characteristics of fibrous capsules of brain abscess were deduced to be due to the presence of heterogeneously distributed free radicals, which were products of respiratory bursts produced by actively phagocytosing macrophages in capsular walls [10].

Although the tumor cells on the edge of the uterine leiomyoma seem to become flattened in the concentric pattern, leading to the clinical impression of a capsule, there is no distinct fibrous capsule microscopically. We usually cannot be observed distinct fibrous capsules of leiomyoma on MR images. Other uterine masses including adenomyosis, leiomyosarcoma, carcinosarcoma, and endometrial stromal sarcoma are not usually accompanied by fibrous capsules because of their infiltrative nature. Pyometra is a collection of pus distending the uterine cavity due to the stenosis of cervical os, and fibrous capsules are not formed by pyometra. Therefore, the fibrous capsules on MR images are expected to be a clue for diagnosis of pyomyoma.

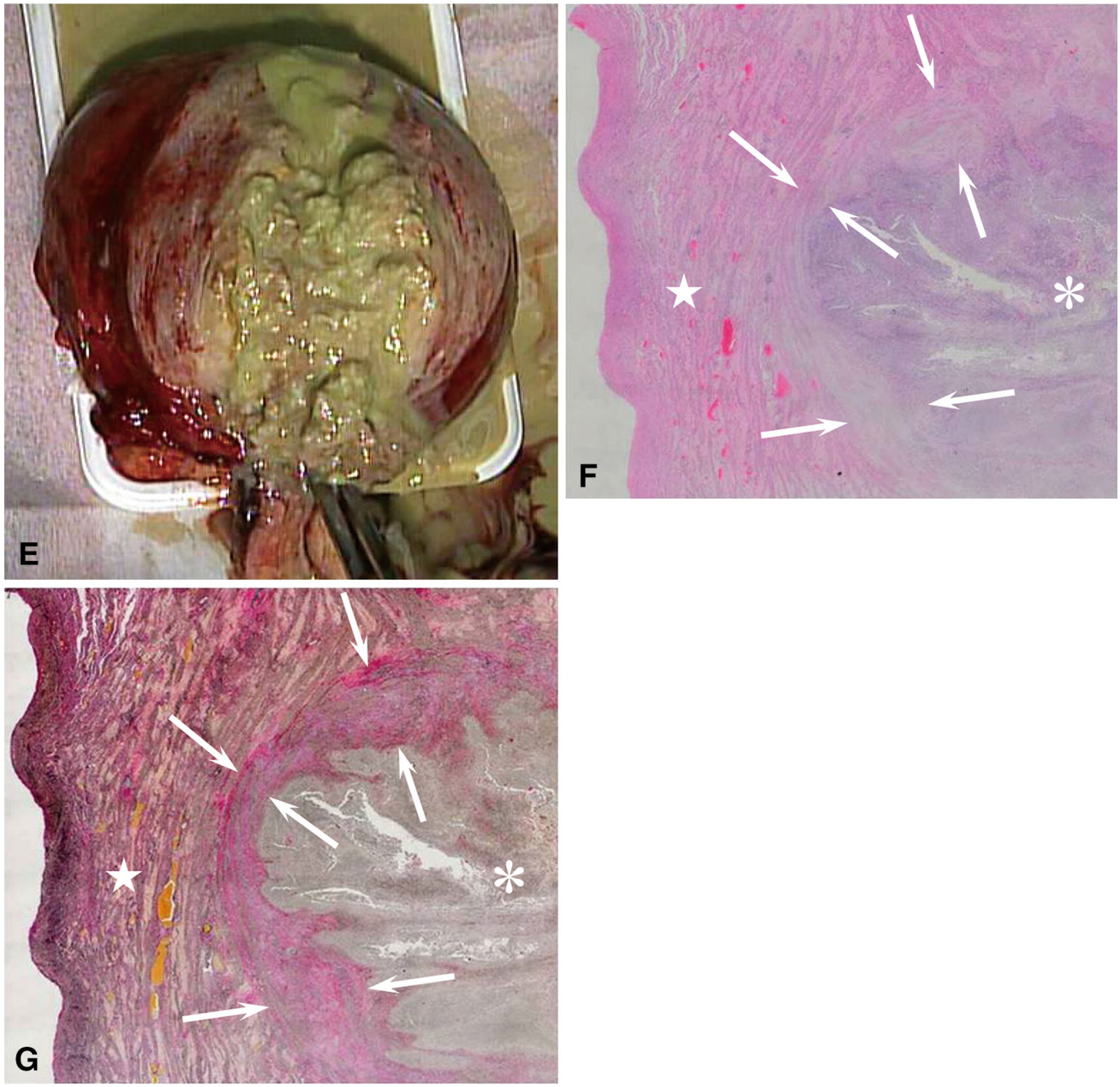

Fig. 1. continued

One radiological differential diagnosis of pyomyoma is leiomyoma with red degeneration. Red degeneration involves a massive hemorrhagic infarction of a leiomyoma caused by the obstruction of drainage veins at the periphery of the lesion [11]. Such degeneration is a type of extensive coagulative necrosis that involves the entire lesion [11]; this condition most often occurs during pregnancy and is also associated with oral contraceptive use. Red degeneration can exhibit peripheral or diffuse hyperintensity on T1-weighted images and variable signal intensity, with or without a hypointense rim, on T2-weighted image [8]. A rim of pyomyoma in present and previous [1] case was demonstrated as a clearly linear structure, whereas a rim of red degeneration usually demonstrates ill-demarcated borders in our experience and the literature review [11, 12]. A peripheral rim, which appeared as hyperintense on T1-weighted images and hypointense on T2-weighted images, of leiomyoma with red degeneration corresponded with numerous dilated vessels filled with red blood cells including intracellular methemoglobin [12]. Although the thrombosed drainage veins prefer to be located at the periphery of leiomyoma, the boundary of these areas with abundant thrombosed vessels is unclear.

The limitation of this case report was that diffusion-weighted MR images were not obtained. In highly vis-

cous fluid, the gross fluid movement velocity is markedly decreased, as is the microscopic diffusional motion of water molecules, which results in low apparent diffusion coefficient (ADC) values. Therefore, the presence of hyperintensity on diffusion-weighted images and low ADC values may suggest the presence of pus within the pyomyoma.

In summary, although the intratumoral gas formation is a clue strongly suggestive of pyomyoma on US and CT imaging, the gas formation is not always observed in pyomyoma as with our case. Because it is difficult to diagnose a pyomyoma without gas formation on US and CT imaging, MR imaging may be useful for the diagnosis of pyomyoma without gas formation by detecting fibrous capsules. The fibrous capsules, which appeared as hyperintense on T1-weighted images and hypointense on T2-weighted images, may be distinctive features that could differentiate pyomyomas from other pathological conditions.

References

1. Kobayashi F, Kondoh E, Hamanishi J, et al. (2013) Pyomayoma during pregnancy: a case report and review of the literature. J Obstet Gynaecol Res 39:383–389.
2. Karcaaltincaba M, Sudakoff GS (2003) CT of a ruptured pyomyoma. AJR Am J Roentgenol 181:1375–1377.
3. Shukla PA, Kumar A, Klyde D, et al. (2012) Pyomyoma after uterine artery embolization. J Vasc Interv Radiol 23:423–424.
4. Fletcher H, Gibson R, Williams N, et al. (2009) A woman with diabetes presenting with pyomyoma and treated with subtotal hysterectomy: a case report. J Med Case Rep 3:7439.
5. Nguyen QH, Gruenewald SM (2008) Sonographic appearance of a postpartum pyomyoma with gas production. J Clin Ultrasound 36:186–188.
6. Lee SR, Kim BS, Moon HS (2010) Magnetic resonance imaging and positron emission tomography of a giant multiseptated pyomyoma simulating an ovarian cancer. Fertil Steril 94:1900–1902.
7. Stroumsa D, Ben-David E, Hiller N, et al. (2011) Severe clostridial pyomyoma following an abortion does not always require surgical intervention. Case Rep Obstet Gynecol 2011:364641.
8. Murase E, Siegelman ES, Outwater EK, et al. (1999) Uterine leiomyomas: histopathologic features, MR imaging findings, differential diagnosis, and treatment. Radiographics 19:1179–1197.
9. Grune B, Zikulnig E, Gembruch U (2001) Sepsis in second trimester of pregnancy due to an infected myoma: a case report and a review of the literature. Fetal Diagn Ther 16:245–247.
10. Haimes AB, Zimmerman RD, Morgello S, et al. (1989) MR imaging of brain abscesses. AJR Am J Roentgenol 152:1073–1085.
11. Ueda H, Togashi K, Konishi I, et al. (1999) Unusual appearances of uterine leiomyomas: MR imaging findings and their histopathologic backgrounds. Radiographics 19: S131–145.
12. Kawakami S, Togashi K, Konishi I, et al. (1994) Red degeneration of uterine leiomyoma: MR appearance. J Comput Assist Tomogr 18:925–928.